

PROPAGATION OF PULSES OVER AN IRREGULAR
AND/OR INHOMOGENEOUS EARTH, COMPARISON
OF THE THEORY AND THE EXPERIMENT

A. AMRI, J. FONTAINE, J. CHANDEZON
CLERMONT-FERRAND II UNIVERSITY
ELECTROMAGNETISM LABORATORY
B.P 45
63170 AUBIERE FRANCE

ABSTRACT

Beyond and direct line-of-sight ground wave propagation measurements were made over two different propagation paths 49 km and 55.4 km in length. Data were collected during the St-Privat d'Allier experimental campaign in 1983 in France. Results presented here include a comparison between measured and predicted pulses. The predictions are based on the paper AMRI et al (1). Measured pulses demonstrated the usefulness of the method developed in this late paper in providing amplitude and wave-form predictions.

INTRODUCTION

The propagation of electromagnetic pulses over an irregular and/or inhomogeneous earth by ground wave is of considerable interest. The introduction of sensitive solid state devices into the industrial plants makes these devices more susceptible to the electromagnetic pulses and, there fore may require additional protection.

In this context, it has become evident that more knowledge regarding the propagation of the electromagnetic pulses is required. Such knowledge can be acquired theoretically by the method developed by the authors in the preceding publication (1). Here, we will compare some of our experimental results obtained in 1983 at the lightning triggering station at St-Privat d'Allier (France) with that obtained theoretically.

THEORY OF PULSE PROPAGATION

We know that the transient field $E(t, r_0)$ at a time t and a distance r_0 on the surface of the earth is related to the continuous time-harmonic solution $E(j\omega, r_0)$, assuming a linear amplitude response of the medium of propagation, by the Fourier transform-integral theorem (6) (2) :

$$E(t, r_0) = \frac{1}{2\pi} \int_{-\infty}^{+\infty} e^{j\omega t} E(j\omega, r_0) M(j\omega) d\omega \quad (1)$$

where $M(j\omega)$ is the Laplace transform of the moment $m(t)$ of the source

$$M(j\omega) = \int_0^{+\infty} m(t) e^{-j\omega t} dt \quad (2)$$

and $E(j\omega, r_0)$ is the ground wave transfer function of the propagation medium, i. e, the solution for the field described by Maxwell's equations for continuous time harmonic wave (1) (2) (3),

$$E(j\omega, r_0) = \frac{1}{4\pi\epsilon_0} \frac{e^{jkr}}{r_0} \left\{ \left(\frac{-2k \cos \theta}{\omega r_0} + \frac{3kar \sin^2 \theta}{\omega r_0^3} \right) \right. \quad (3)$$

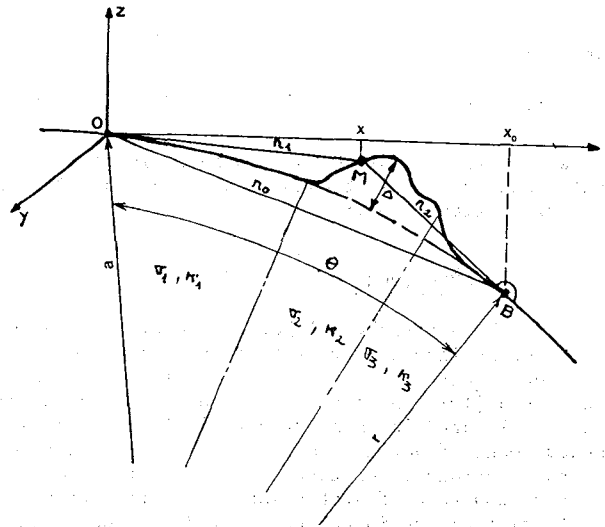
$$\left. -j \left(\frac{2 \cos \theta}{\omega r_0^2} + \frac{1}{\omega r_0^2} (k^2 ar \sin^2 \theta) + \frac{1}{\omega r_0^4} (-3arsin^2 \theta) \right) \right\}$$

$$x \quad W(j\omega, r_0)$$

k being the propagation constant, ϵ_0 is the permittivity of free space and ω is the angular frequency. The quantities r_0, r_1, r_2, r and θ are shown on figure 1.

$W(j\omega, r_0)$ is the attenuation function defined by (5) (3),

$$W(j\omega, x_0) = 1 - e^{-j \frac{\pi}{4} \left(\frac{k}{a\pi} \right)^{1/2} \int_0^{x_0} \left(\frac{x_0}{x(x_0-x)} \right)^{1/2} W(j\omega, x) \left(\delta + \left(1 + \frac{j}{kr_2} \right) \frac{\partial r_2}{\partial n} \right) e^{jk(r_1+r_2-r_0)} dx} \quad (4)$$



- Figure 1 -

Where x and x_0 are projections of r_1 and r_0 on the $z = 0$ plane and δ is defined by :

$$\delta = \left(\kappa + j \frac{\sigma}{\omega \epsilon_0} \right)^{-1/2} \quad (5)$$

κ and σ are respectively the dielectric constant and the conductivity of the earth.

In equation (4), δ accounts for the imperfect conductivity of the earth and the function $\partial r_2 / \partial n$ accounts for its irregular topography.

The moment $m(t)$ of the source can be correctly modeled and the corresponding field $E(t, r_0)$ may be

accordingly predicted (1). If we possess a recording of the signal $E(t, d_1)$ at a distance d_1 from the source, by means of the transfer function of the medium $E(j\omega, d_1)$ we can determine the spectrum $S(j\omega)$,

$$S(j\omega) = \frac{F(j\omega, d_1)}{E(j\omega, d_1)} \quad (6)$$

which is the spectrum of the source. $F(j\omega, d_1)$ is defined by :

$$F(j\omega, d_1) = \int_0^{\infty} e^{-j\omega t} E(t, d_1) dt \quad (7)$$

The signal $E(t, d_2)$ at a distance d_2 from the source can be predicted by :

$$E(t, d_2) = \frac{1}{2\pi} \int_{-\infty}^{+\infty} S(j\omega) E(j\omega, d_2) e^{-j\omega t} d\omega \quad (8)$$

where $E(j\omega, d_2)$ is the transfer function of the medium between the source and the observer at distance d_2 . The quantities $E(j\omega, d_1)$ and $F(j\omega, d_2)$ are defined by the equation (3).

The inverse Fourier transform (8) can be approximated by the following discrete transform (9) :

$$E(pT_1, d_2) = \frac{1}{T} \sum_{n=0}^{N-1} E(jn\omega_0, d_2) \frac{F(jn\omega_0, d_2)}{E(jn\omega_0, d_1)} e^{jn\omega_0 pT_1} \quad (9)$$

where :

$$T_1 = T/N \quad \omega_0 = 2\pi/T \quad p = 0, 1, 2, \dots, N-1$$

This discrete transform (9) can be evaluated in a computationally efficient manner using the fast Fourier transform algorithm (8)

EXPERIMENT SET

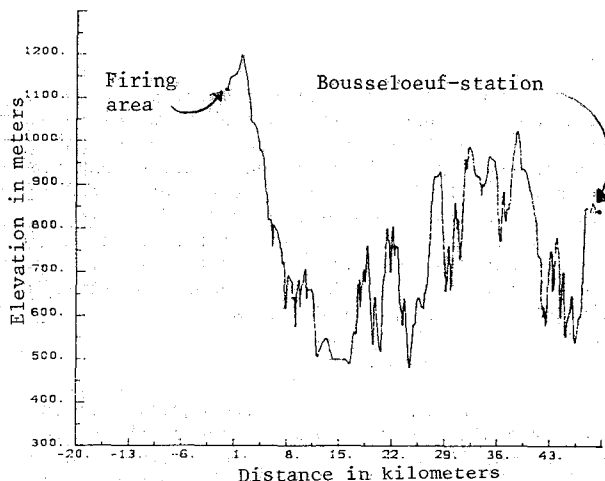
The artificial triggered lightning discharges are made by launching rockets towards the storm cloud. The rocket unrolls behind it a metallic wire connected to ground (10). The layout of a rocket launching platform is located in Saint-Privat d'Allier (France). The measurement of vertical electric field was carried out at two stations at distances respectively of 49 kilometers (Busseloef-station) and 55.4 kilometers (Laurie-station) from the launching site. Busseloef-station was installed beyond line-of-sight, i.e, with the receiving antenna below the radio horizon in the so-called diffraction region. Laurie-Station was installed on Hertzian tower, thus on high point within optical range of the launching site. Both stations were equipped with a recording system which comprised a measuring chain composed of :

- two modified commercial rotating head recorders (video-recorders) having a 2 Megahertz pass-band.
- an electric pick-up
- an electronic clock for comparison of signals

The electric field pick-ups are composed of a dipole antenna followed by a capacitive divider and by a wide band amplifier (300 Hz-10MHz) with a symmetrical input (4). Under these conditions, rise time (10% - 90%) was estimated with a precision greater than 0.2 microseconds.

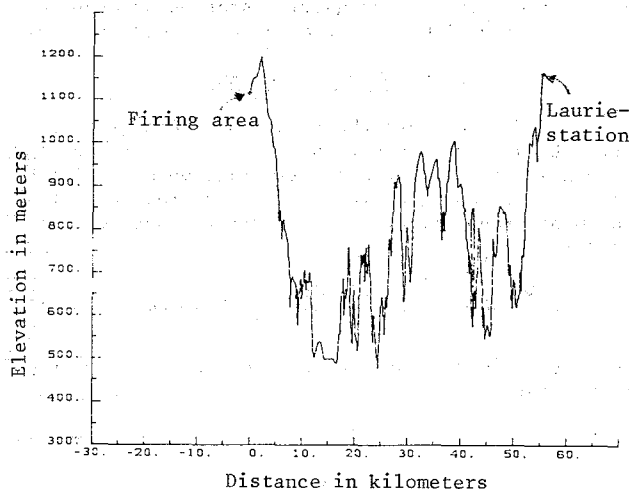
PROPAGATION PATH DESCRIPTION

Measurements of received signals were made for two different propagation paths. The profile of the first path which corresponds to the terrain between the firing area and Busseloef-station is shown on figure 2 and that which corresponds to the second path, i.e, to the profile of the terrain between the firing area and Laurie-station is shown on figure 3.



- Figure 2 -

Propagation path profile corresponding to the terrain between the firing area and Busseloef-station



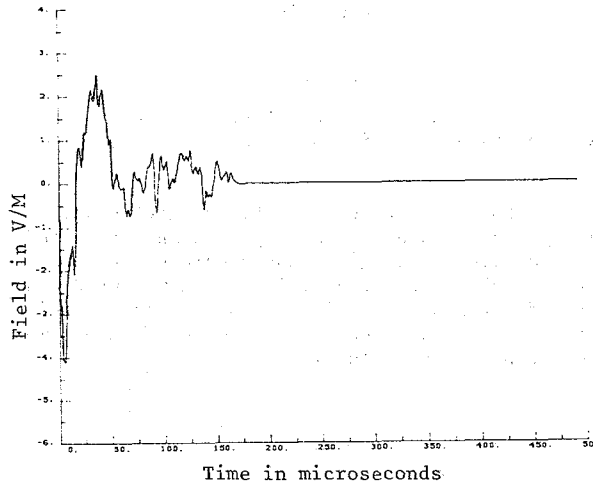
- Figure 3 -

Propagation path profile corresponding to the terrain between the firing area and Laurie-station

Both profiles are composed of a three sections. In the first path the lengths of the three sections are respectively 14.15 km, 2.7 km and 32.2 km. In the second path the lengths of the three sections are respectively of 14.15 km, 2.7 km and 38.55 km. The conductivity and the permittivity of the first and the third sections of both profiles are the same and are equal respectively to $\sigma = 0.005$ mho/m and $\kappa = 13$. The second section of both profiles is characterised by $\sigma = 0.002$ mho/m and $\kappa = 5$.

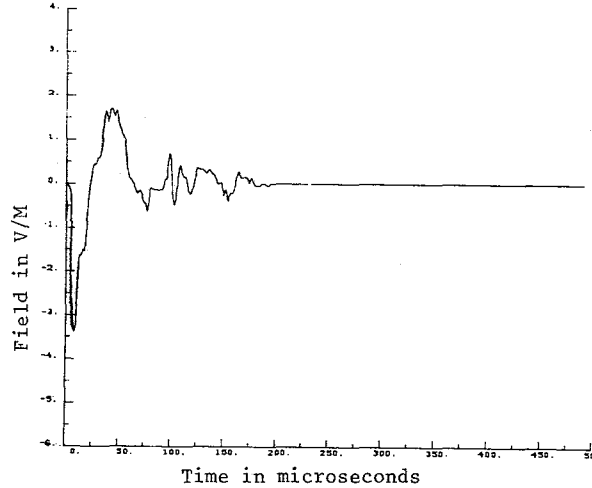
MEASUREMENTS

The summer 1983 was poor in thunderstorms. Only one triggered lightning (number 8301) was rich in return stroke. The wave shapes of vertical electric fields recorded at Busseloef-station and Laurie-station are shown respectively on figures 4 and 5. These pulses correspond to the most significant results in the triggered lightning number 8301.



- Figure 4 -

Vertical electric field due to the first return stroke (firing 8301), measured at Busseloef-station

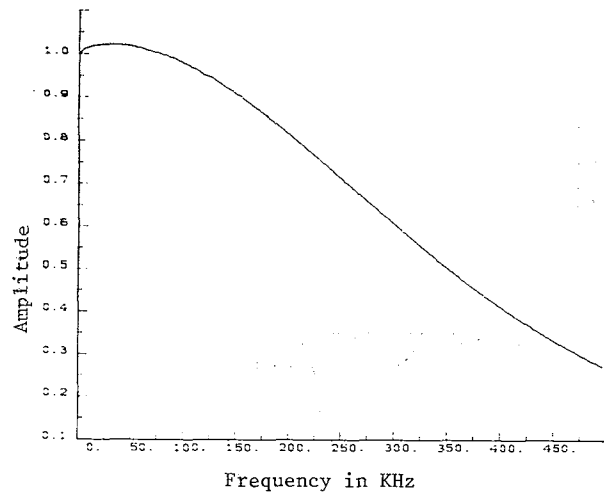


- Figure 5 -

Vertical electric field due to the first return stroke (firing 8301) measured at Laurie-station

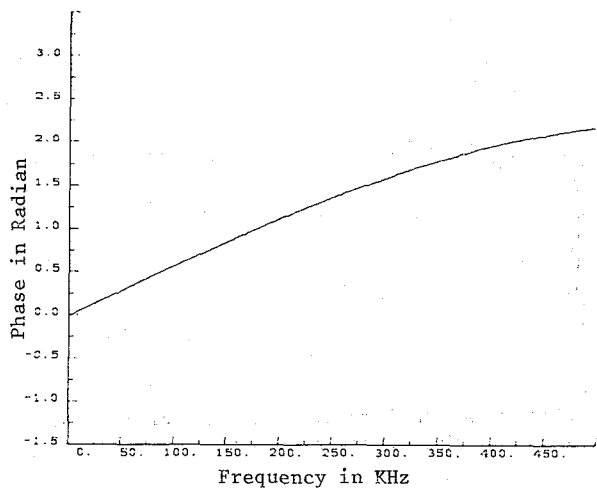
RESULTS OF THE CALCULATION

In figures 6 and 7 calculations are given of the amplitude and phase of the attenuation function W versus frequency for the first path (fig.2)



- Figure 6 -

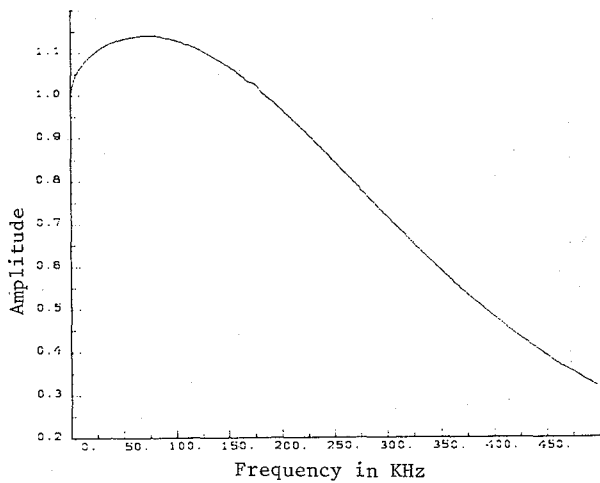
Amplitude of the ground-wave attenuation function W ($j\omega, 49\text{km}$) as a function of frequency ($\sigma_1 = \sigma_3 = 0.005$; $\kappa_1 = \kappa_3 = 13$; $\sigma_2 = 0.002$; $\kappa_2 = 5$) for the first path.



- Figure 7 -

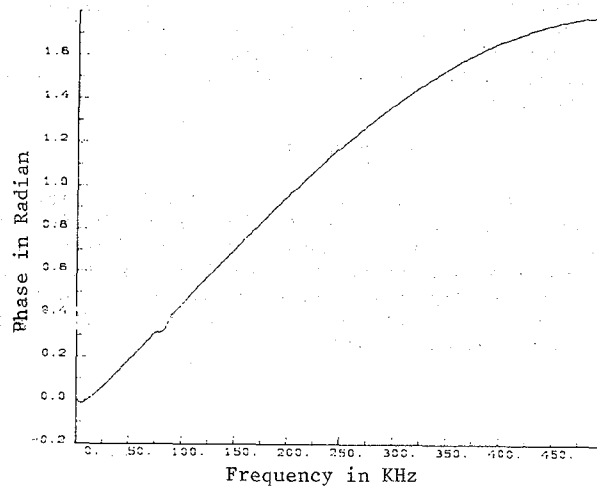
Phase of the ground wave attenuation functions for the first profile with $(\sigma_1 = \sigma_3 = 0.005 ; \kappa_1 = \kappa_3 = 13 ; \sigma_2 = 0.002 \text{ et } \kappa_2 = 5)$

The amplitude and phase of the attenuation function corresponding to the second path are shown respectively on figures 8 and 9.



- Figure 8 -

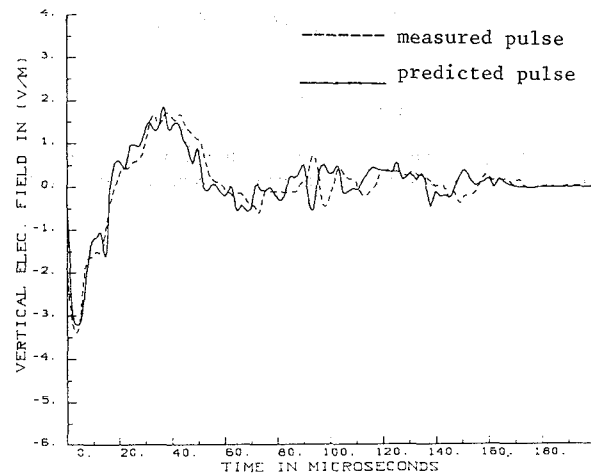
Amplitude of the ground wave attenuation function $W(j\omega, 55.4 \text{ km})$ as a function of frequency



- Figure 9 -

Phase of the ground wave attenuation function $W(j\omega, 55.4)$ as function of frequency

Starting from the recording at Bousseloef-station (fig.4), the formula (9), which has been translated into a computer code, gives the predicted vertical electric field at Laurie-station. Both measured and predicted vertical electric fields are shown on figure 10 in which a good agreement can be seen between measured and predicted values.



- Figure 10 -

Measured and predicted vertical electric fields at Laurie-station

CONCLUSION

While the transient response was illustrated explicitly for one of the return stroke models and an irregular earth in the preceding paper (1), the present analysis extends the results in the case where the original pulse is an observed one. The comparison between measured and predicted pulses demonstrates the usefulness of our method in providing amplitude and waveform predictions.

ACKNOWLEDGEMENT

This work was supported by Le Commissariat à l'Energie Atomique (C.E.A.). The various sensors and recording system were adapted to our requirements by Le Laboratoire de Geophysique LDG/CEA.

REFERENCES

- (1) A. AMRI, J. CHANDEZON, J. FONTAINE, Propagation of pulses over an irregular and/or inhomogeneous earth, IEEE, 1984 International EMC Record Number : 84 - CH2097-4, vol-1, 479-482, 1984.
- (2) A. AMRI, J. CHANDEZON, J. FONTAINE, Propagation d'impulsions électromagnétiques sur une terre irrégulière et/ou non-homogène, Proceedings of the National symposium on the EMC, Clermont-Ferrand (France), 19-21 June 1985.
- (3) A. AMRI, J. FONTAINE, J. CHANDEZON, Quantification d'erreurs inhérentes au formalisme intégral relatif à l'étude de la propagation de l'onde de sol, Proceedings of the National symposium on the EMC, Clermont-Ferrand(France), 19-21 June 1985.
- (4) J. HAMELIN, A. MEESTERS, Mesure des champs électromagnétiques créés par les décharges orageuses, Proceedings of the international symposium on measurements in telecommunications, 530-536, Lannion (France), 3-7 oct. 1977.
- (5) G.A. HUFFORD, An integral equation approach to the problem of wave propagation over an irregular surface, Quart. Appl. Math., 9, 391-403, 1952.
- (6) J.R. JOHLER, Propagation of the low-frequency radio signal, Proc. of the IRE, n°4, 404-427, 1962.
- (7) J.R. WAJT, On the Electromagnetic pulse response of a dipole over a plane surface, Can. J. Phys., 52, 193-196, 1974.
- (8) R.C. SINGLETON, An algorithm for computing the mixed radix FFT, IEEE, Trans. Audio - Electroacoust, vol. AU-1, n°2, 93-107, 1969.
- (9) A. PAPOULIS, Signal analysis, New-York : Mc Graw-Hill, 1977, ch.3, pp. 56-91.
- (10) FIEUX R.P., C.H. GARY, B.P. HUTZLER, A.R. EYBENT-BERARD, P.L. HUBERT A.C. MEESTERS, P.H. HAMELIN and J.M. PERSON, Research on Artificially Triggered Lightning in France, I.E.E.E. Trans. Power Apparatus Syst., PAS-97,725-733, 1978.